Hydrobiologia (2011) 675:105–117
DOI 10.1007/s10750-011-0807-0

PRIMARY RESEARCH PAPER

Solar ultraviolet radiation and CO_2-induced ocean acidification interacts to influence the photosynthetic performance of the red tide alga *Phaeocystis globosa* (Prymnesiophyceae)

Shanwen Chen · Kunshan Gao

Received: 1 March 2011 / Revised: 31 May 2011 / Accepted: 18 June 2011 / Published online: 1 July 2011

Abstract Future CO_2-induced ocean acidification may interact with solar UV radiation to affect physiological performance of microalgae. Therefore, CO_2/pH perturbation experiments were carried out under solar radiation with or without UV radiation (295–400 nm) to evaluate the combined effects of seawater acidification (pH 7.7 at 101.3 Pa CO_2) and UV on *Phaeocystis globosa* that forms harmful algal blooms. Under high levels of solar radiation, the acidification reduced the growth rate and photochemical efficiency either under PAR alone or with the presence of UVR radiation. Under reduced levels of solar radiation (cloudy days), however, the CO_2-enrichment and UVA acted synergistically to stimulate the photochemical yield and enhanced the growth rate. That is, the effects of CO_2-induced acidification were reversed from the negative (sunny days) to positive (cloudy days). CO_2 concentrating mechanism f *P. globosa* was not affected by the elevated pCO_2 in view of unchanged photosynthetic affinity for CO_2 and stable activity of both intracellular and extracellular carbonic anhydrase. The increased acidity induced higher UVB-related photoinhibition of growth and non-photochemical quenching, and increased the dark respiration and the contents of Chl *a*, Chl *c*, and carotenoids, causing the cells to increase their energy demand against the combined stress. Overall, the findings imply that net or balanced effects of ocean acidification on phytoplankton would depend on the depth or mixing that alters the exposures of the cells in water columns to solar radiation.

Keywords CO_2 · Growth · Ocean acidification · *Phaeocystis globosa* · Photochemical yield · UV

Abbreviations

PAR	Photosynthetically active radiation
PSII	Photosystem II
UVA/B/R	Ultraviolet-A/-B/radiation
P	PAR alone
PA	PAR + UVA
PAB	PAR + UVA + UVB

Introduction

Increasing levels of the atmospheric CO_2 and ultraviolet B radiation (UVB: 290–320 nm), as a result of industrial activities, may cause unprecedented changes in marine ecosystems (Beardall et al., 2009). Increasing

Handling editor: Luigi Naselli-Flores

S. Chen
Marine Biology Institute, Shantou University, Shantou 515063, China

K. Gao (✉)
State Key Laboratory of Marine Environmental Science, Xiamen University, Xiamen 361005, China
e-mail: ksgao@xmu.edu.cn

pCO_2 in seawater, may enhance marine primary production (Hein and Sand-Jensen 1997; Schippers et al., 2004), alter phytoplankton community structure (Tortell et al., 2002) and stimulate biological carbon consumption (Riebesell et al., 2007). However, such a CO_2-related enhancement has been suggested not to be significantly important, since most phytoplanktonic species examined so far possess CO_2 concentration mechanisms (CCMs) (Raven & Beardall, 2003; Giordano et al., 2005). Nevertheless, CO_2 enrichment usually down-regulates the capability of CCMs (Burkhardt et al., 2001; Rost et al., 2003; Giordano et al., 2005), while presence of UV radiation (UVR, 290–400 nm) affects the CO_2 acquisition and CCMs in phytoplankton species (Beardall et al., 2002; Sobrino et al., 2005; Wu & Gao, 2009). However, little has been documented on the compounded effects of CO_2-induced seawater acidification and UVR on marine phytoplankton (Sobrino et al., 2008; Gao et al., 2009).

Continuous dissolution of CO_2 from the atmosphere into the seawater has been causing ocean acidification, leading to increased concentrations of HCO_3^- and H^+ and a decrease in the concentration of CO_3^{2-} and the saturation state of calcium carbonate (Caldeira & Wickett, 2003; Orr et al., 2005). The surface seawater will be acidified by 0.3 to 0.4 units (about a 100–150% increase of H^+) by 2100 (Caldeira & Wickett, 2003) at the projected atmospheric CO_2 level of 800–1000 ppmv (81.0–101.3 Pa) under the 'business-as-usual' CO_2 emission scenario (Orr et al., 2005). It is known that the ocean acidification reduces calcification of marine calcifiers (Gao et al., 1993; Riebesell et al., 2000; Hoegh-Guldberg et al., 2007) and can even influence the olfactory sensing of fish (Munday et al., 2009). However, it is unknown what would take place in the future oceans to the non-calcifying photosynthetic organisms that drive the marine biological CO_2 pump. In addition, little is known about the physiological response of red tide species to ocean acidification, which is important for prediction of future harmful algal blooms (HAB).

Solar UV radiation affects photosynthetic carbon fixation (Helbling et al., 2003; Gao et al., 2007b; Lesser 2008), damages DNA (Buma et al., 2006; Gao et al., 2008) and proteins (Bouchard et al., 2005) and even alters morphology (Schmidt et al., 2010) of photosynthetic organisms. On the other hand, UVA (320–400 nm) is known to stimulate photosynthetic carbon fixation (Helbling et al., 2003; Gao et al., 2007b) of phytoplankton assemblages and enhance the activity of carbonic anhydrase that facilitates bicarbonate utilization in a diatom (Wu & Gao, 2009). Since UVR can affect photosynthetic CO_2 fixation in different ways, it may interact with ocean acidification to affect marine primary producers. Therefore, it is of general interest to see if changes in seawater carbonate system and UVR would act synergistically, antagonistically or independently on phytoplankton species. The ongoing increase of pCO_2 and acidity in surface oceans due to increasing atmospheric CO_2 may alter physiological responses of phytoplankton to UVR. Recently, it has been shown that UVR brings more harm to a coccolithophorid (Gao et al., 2009) and coralline alga (Zheng & Gao, 2009) under CO_2-induced seawater acidification. However, how UV and ocean acidification would interact to affect algal species that form harmful blooms remains unknown.

Phaeocystis globosa is one of the heteromorphic marine phytoplankton, displaying gelatinous colonies as well as flagellated solitary cells (Rilegman and Boekel, 1996). This organism frequently forms HAB from the North Sea to the South China Sea (Qi et al., 2004; Schoemann et al., 2005; Peperzak & Poelman, 2008). The aim of this study is to investigate the responses of *P. globosa* to solar radiation with or without UVR under ambient and elevated CO_2 concentrations in order to understand the combined effects of solar UVR and CO_2-induced ocean acidification.

Materials and methods

Organism and culture conditions

Phaeocystis globosa Scherffel (ST-97) was isolated during its bloom occurred in the Southern China Sea in 1997 and obtained from Xiamen University. An axenic culture was maintained in modified f/2 medium under indoor conditions at 50 μmol photons m^{-2} s^{-1} (PAR) (12L:12D) and 15°C. We chose the flagellated form for this study since it accounts for most of the time during the life cycle of *P. globosa* and is responsible for the occurrence of HAB (Rousseau et al., 2007). The flagellated cells (3–6 μm) had been grown for 3 days (about 9 generations) at their exponential growth phase under

the full solar radiations at 20°C before being used for the high CO_2/low pH perturbation experiments.

CO_2/pH perturbation treatments

Since photosynthetic carbon fixation often exceeds dissolution (hydration) of CO_2 from aeration in algal cultures, resulting in pH rise even under elevated CO_2 levels (Gao et al., 1991), the best way to maintain constant pH level is to use continuous or semi-continuous cultures, while maintaining low cell concentration (LaRoche et al., 2010). We operated turbidostatic cultures from May 01 to May 08, 2009 under solar radiation and the cell concentration was maintained within a range of 0.9–1.1 $\times$ 10^5 cells ml^{-1}. The flow rates (efflux from and influx to the culture) were adjusted in order to maintain a stable cell concentration and carbonate system. During the night period, the cell density in the culture was adjusted to a proper value before the renewal (flow) was terminated at 24:00 so that the cell concentration reached about 1.0 $\times$ 10^5 cells ml^{-1} at 6:00 next morning when the flow was resumed. The turbidostatic culture system consisted of a culture vessel (a quartz tube of 1200 ml, 7.0 cm in diameter and 40 cm in length), a medical transfusion unit for transfusing the medium and adjusting the flow rate. CO_2 enrichment with aeration is one of the several techniques recommended for pH perturbation experiments (Gattuso and Lavigne 2010). In this study, aeration rate was adjusted within a range of 700–900 ml min^{-1} in order to maintain the stability of the seawater carbonate chemistry (Table 1) under changing solar radiation. Filters (SLLG013SL, Millipore, USA) of 0.2-μm-pore size were used to filter the aerating air with or without the CO_2 enrichment. A total of 18 culture sets (triplicate at each treatment, 2 CO_2 levels and 3 radiation treatments) were operated at the same time for repetition. The pH in the cultures was measured with a pH-meter (Seveneasy, Mettler-Toledo, Switzerland), which was frequently calibrated with standard N. B. S. buffer solution (Merck, Germany). The quartz tubes, which allow penetration of UV, were maintained in a water bath for temperature control at 20 ± 1°C using a refrigerated circulator (CAP-3000, Tokyo Rikakikai, Japan).

The CO_2-enriched (101.3 Pa CO_2) air was pumped from a CO_2 chamber (Conviron EF7; Controlled Environments Limited, Canada), in which the CO_2

Table 1 Parameters of the seawater carbonate system under the ambient (39.3 Pa) and enriched (101.3 Pa) CO_2 levels in the turbidostatic cultures under different radiation treatments with (PA, PAR + UVA; PAB, PAR + UVA + B) or without (P, PAR) UVR

	39.3 Pa CO_2			101.3 Pa CO_2		
	P	PA	PAB	P	PA	PAB
pH	8.08 ± 0.02^{a}	8.07 ± 0.03^{a}	8.07 ± 0.03^{a}	7.71 ± 0.03^{b}	7.70 ± 0.02^{b}	7.70 ± 0.02^{b}
DIC (μmol kg^{-1})	2016.1 ± 94.3^{c}	2009.4 ± 102.6^{c}	2016.8 ± 106.2^{c}	2182.9 ± 107.1^{d}	2181.3 ± 101.4^{d}	2179. 4 ± 111.3^{d}
HCO_3^- (μmol kg^{-1})	1842.9 ± 87.8^{e}	1842.1 ± 79.6^{e}	1846.3 ± 91.2^{e}	2063.7 ± 91.5^{f}	2064.6 ± 101.3^{f}	2063.1 ± 98.0^{f}
CO_2aq (μmol kg^{-1})	16.6 ± 0.6^{g}	16.9 ± 0.4^{g}	17.1 ± 0.5^{g}	44.2 ± 0.7^{h}	45.3 ± 0.9^{h}	44.5 ± 0.8^{h}
CO_3^{2-} (μmol kg^{-1})	154.1 ± 26.5^{p}	151.8 ± 31.2^{p}	150.9 ± 29.1^{p}	73.9 ± 24.6^{q}	71.8 ± 19.6^{q}	72.6 ± 21.5^{q}
TA (μmol kg^{-1})	2221.3 ± 97.1^{m}	2215.6 ± 103.0^{m}	2219.2 ± 93.5^{m}	2241.6 ± 112.2^{n}	2243.1 ± 96.4^{n}	2241.3 ± 101.3^{n}
TA_m (μmol kg^{-1})	2283.1 ± 102.0^{m}	2279.4 ± 111.3^{m}	2280.6 ± 112.2^{m}	2296.5 ± 117.4^{n}	2299.7 ± 100.7^{n}	2279.8 ± 117.0^{n}

Dissolved inorganic carbon (DIC), pH, salinity (33‰), nutrient concentration (Phosphate, 3.6; Silicate, 11.3 μmol/kg-SW), and temperature (20°C) were used to derive all other parameters using a CO_2 system analyzing software (CO2SYS). The stoichiometric equilibrium constants K_1 and K_2 for carbonic acid are 6.04 and 9.16, respectively. Each datum represents the mean ± SD (n = 24) except that of the measured TA (TA_m) values in parentheses (n = 9). Different superscript letters indicate significant differences

concentration was automatically achieved by mixing pure CO_2 and the ambient air (39.3 Pa CO_2). This CO_2 level agrees with recommendations by Barry et al. (2010) for ocean acidification research. The acidity of the seawater medium was maintained at pH 8.07 for the ambient and at 7.70 for the CO_2-enriched treatment, with variations less than 0.03 (Table 1).

Solar radiation monitoring and treatments

Incident solar radiation was continuously monitored with an ELDONET radiometer (Real Time Computer, Möhrendorf, Germany). This instrument has 3 irradiance channels, respectively, for photosynthetically active radiation (PAR, 400–700 nm), UVA (UVA, 315–400 nm) and UVB radiation (UVB, 280–315 nm). Its reliability has been internationally recognized (Häder et al., 1999), being certificated with having the homologous error less than 0.5% in comparison with the most accurate instrument (certificate No. 2006/BB14/1). The device is calibrated regularly with the support from the maker against a double monochrometor spectroradiometer and a certified calibration lamp. It was installed at a roof of Shantou University (23.3°N, 116.6°E), where the cultures were operated under the sun.

The cells were exposed to three radiation treatments: (a) PAR + UVA + UVB (PAB), quartz tubes covered with Ultraphan 295 film (Digefra GmbH, Munich, Germany), receiving solar irradiances above 295 nm; (b) PAR + UVA (PA), covered with Folex 320 (Folex GmbH, Dreieich, Germany), receiving irradiances above 320 nm; and (c) PAR alone (P), covered with Ultraphan 395 (Digefra GmbH, Munich, Germany), receiving the light above 395 nm. The transmission spectra of the cut-off filters have been published elsewhere (Zheng & Gao, 2009). The cut-off filters reduce 4% of PAR (Gao et al., 2007a) in water due to their reflections. There were about 5 nm differences between the measured and exposed UVA waveband and 5 nm differences between the measured and exposed UVB. Therefore, the cells received about 2% less UVA, 0.3% less UVB irradiance and about 4% less PAR in contrast to the measured irradiances.

Assessment of photochemical activity

Chlorophyll fluorescence parameters indicative of photochemical activity were determined with a pulse amplitude modulated fluorometer (WATER-PAM, Walz, Germany). The effective quantum yield ($\Delta F/F'_m$) was determined on the basis of the instant maximal fluorescence (F'_m) and the steady-state fluorescence (F_t) of the light-adapted cells according to Genty et al. (1989): $\Delta F/F'_m = \left(F'_m - F_t\right)/F'_m$. The nonphotochemical quenching (NPQ) was determined on the basis of the maximal fluorescence (F_m) of the dark-adapted cells at 6:00 (before the sun rise) and the instant maximal fluorescence (F'_m) of the light-adapted cells during daytime as follows: $NPQ = \left(F_m/F'_m\right)/F_m$ (Bilger & Björkman, 1990). In the course of measuring F_m, F'_m and F_t, the saturating pulse (0.8 s) and actinic light were set at 4000 and 150 μmol photons m^{-2} s^{-1}, respectively.

Determination of photosynthesis and respiration

Photosynthetic oxygen evolution and dark respiration were measured with a Clark-type O_2 electrode (YSI 5300; Yellow Springs Instrument Co., Inc., Yellow Springs, USA). The cells grown at the low or high CO_2 levels for at least 9 generations were incubated and their photosynthesis/respiration was measured in the seawater equilibrated with different levels of CO_2 under PAR of 400 μmol photons m^{-2} s^{-1} or complete darkness.

Determination of growth rate

Since the cultures were operated continuously from 06:00 to 24:00 and non-continuously from 24:00 to 06:00, the specific growth rate (μ) was calculated as: $\mu = F/V + (\ln D_e - \ln D_0)$, where F represents the sum of the effluent and samples taken during the period of 06:00 to 24:00; V, the volume of the culture; D_0 and D_e represent, respectively, cell densities at the start (24:00) and the end (6:00) of the period during which the medium was not renewed.

Determinations of photosynthetic pigments and UV-absorbing compounds

Pigments and UV-absorbing compounds (UVACs) of about 1.0×10^7 cells were determined by filtering 100 ml culture through a Whatman GF/F filter, extracting in 5 ml absolute methanol overnight and centrifuging for 10 min (2000 g) at 4°C, and measuring the

absorption of the supernatant with a spectrophotometer (DU_{530} DNA/Protein Analyzer, Beckmen Coulter, USA) as previously reported (Gao et al., 2007a). Chl *a*, Chl *c*, carotenoids were calculated according to Wellburn (1994). The absorption peak at 340 nm was used to estimate total absorptivity of UVACs according to Dunlap et al. (1995).

Assessments of carbonic anhydrase activity

Samples taken during noon period (12:00–12:10) were used to determine the activities of carbonic anhydrase (CA). Total CA activity (periplasmic extracellular and intracellular CA: ECA and ICA) was determined according to Ye et al. (2008). Briefly, 10-ml sample was centrifuged for 10 min at 2000 g and 4°C, and the pellet was resuspended in 4 ml (4°C) of assay buffer [pH 8.4, 20 mmol l^{-1} Veronal, 5 mmol l^{-1} EDTA, 2.5 mM DTT, 2% (w/v) PVP-40, 0.1% (w/v) Triton X-100 and 0.5% (w/v) BSA]. The time required for the pH drop from 8.2 to 7.2 after addition of 1 ml of cold (4°C) CO_2-saturated water was recorded to calculate the activity of CA. The intact cells and the ruptured (homogenized) cells were used to determine the ECA and total CA, respectively. The ICA was obtained as the difference between the total CA and ECA.

Measurements of dissolved inorganic carbon and total alkalinity

Dissolved inorganic carbon (DIC) was measured using a total carbon analyzer (TOC-5000, Shimadzu, Japan), which automatically measured DIC and TC in the supernatant (after centrifugation). Total alkalinity (TA) was measured according to Anderson & Robinson (1946). Other parameters for the seawater carbonate system were estimated according to the measured values of DIC and pH using the software CO_2SYS (Lewis & Wallace, 1998) (Table 1).

Data analysis

UV-induced inhibition was assessed as:

$$\mathrm{UVA_{Inh}}(\%) = ((X_P - X_{PA})/X_P) \times 100$$

$$\mathrm{UVB_{Inh}}(\%) = ((X_{PA} - X_{PAB})/X_P) \times 100$$

where $\mathrm{UVA_{Inh}}$ and $\mathrm{UVB_{Inh}}$ represent UVA and UVB-induced inhibition, X_P, X_{PA}, and X_{PAB}, the specific growth rate (μ) or effective quantum yield ($\Delta F/F_m$) of the cells grown under PAR alone, PAR + UVA and PAR + UVA + UVB treatments, respectively.

Paired *t* test was used to establish the significant difference among the treatments at $P < 0.05$.

Results

Radiations, temperature, pCO_2, DIC, pH, and TA

When *P. globosa* cells were cultured under different solar radiation treatments at pH 8.07 (39.3 Pa CO_2) or pH 7.70 (101.3 Pa CO_2), daily doses of solar radiation ranged 2.34–6.73 for PAR, 0.39–1.06 for UVA and 0.01–0.03 MJ m^{-2} for UVB (Fig. 1a). The noontime irradiances were 112.3–279.6 for PAR, 18.8–43.1 for UVA and 0.6–1.4 W m^{-2} for UVB, respectively. The daytime average PAR level was

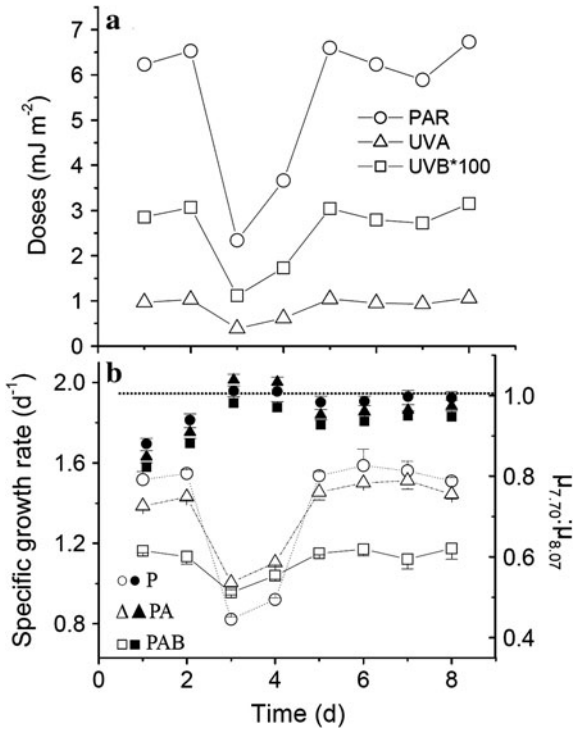

Fig. 1 **a** Daily doses of solar PAR, UVA, or UVB durng the culture period of May 1–8, 2009. **b** Specific growth rates (*open symbols*) of *Phaeocystis globosa* grown at pH 8.07 and the ratios (*solid symbols*) of the specific growth rate at pH 7.70 to that at pH 8.07 ($\mu_{7.70}$:$\mu_{8.07}$) under solar PAR (P), PAR + UVA (PA) or PAR + UVA + UVB (PAB), respectively. The data represent the mean ± SD in triplicate cultures ($n = 3$)

150.3 on the sunny days, and 67.8 W m^{-2} on the cloudy or rainy days. The ratio of UVB to PAR ranged from 0.45 to 0.48%; whereas that of UVA to PAR from 15.2 to 16.8%. Changes in the cloud cover regulated the variation in the solar radiation levels. The ozone concentration in the stratosphere over the experimental site during the period varied from 271 to 317 DU (http://jwocky.gsfc.nasa.gov/), which negatively correlated with the measured UVB irradiance or UVB to PAR ratio. DIC, CO_2aq, and HCO_3^- were, respectively, 8.1, 164.8, and 11.9% higher, and CO_3^{2-} 52.2% lower in the CO_2-enriched cultures compared to the control (Table 1). The pH was significantly reduced ($P < 0.01$) by 0.37 units in the high CO_2 cultures, and changed insignificantly ($P > 0.1$) under the different radiation treatments with or without UVR (Table 1).

Growth

The specific growth rates varied with changes in solar radiation, being higher on the sunny days and lower at the cloudy/rainy days. At pH 8.07 (the ambient CO_2 level), it ranged 1.51–1.59 (P), 1.39–1.51 (PA) and 1.12–1.17 day^{-1} (PAB) on the sunny days and 0.82–0.92 (P), 1.01–1.11 (PA), and 0.96–1.04 d^{-1} (PAB) on the cloudy/rainy days, respectively (Fig. 1b). It appeared that presence of UVA inhibited the growth on the sunny days, but enhanced it on the cloudy/rainy days. The lowest growth rate was observed at day 3 when the solar radiation was the lowest. During the initial period (2 days), the growth rate was, on average, depressed by 11.5% (under PAR), 12.8% (under PAR + UVA) and 13.7% (under PAR + UVR) in the high CO_2/low pH cultures as reflected in the ratios of $\mu_{8.07}$ to $\mu_{7.70}$ ($P < 0.05$), in comparison to those in the low CO_2/high pH cultures. On the cloudy/rainy days (day 3 and 4), however, the CO_2 enrichment enhanced the growth rate by 1.1–2.3% under PAR and 2.9–4.1% under PAR + UVA ($P < 0.05$), and inhibited it by 1.9–3.0% ($P < 0.05$) under PAR + UVA + B. On the sunny days from day 5 to day 8, the acidification reduced the growth rate by 0.6–1.7% under PAR, 2.7–4.8% under PAR + UVA and by 5.0–7.3% under PAR + UVA + B. Presence of UVA or UVB significantly inhibited the growth rate on the sunny days by up to 5.1 or 17.5% at the high pH and by up to 7.8 or 22.0% at the low pH level, respectively ($P < 0.05$) (Fig. 2). On the cloudy/rainy days (day 3 and 4) when solar radiation were low, presence of UVA significantly enhanced the growth rate by 24.6–26.0% at the high pH and by 28.7–29.7% at the low pH level; UVB reduced the growth rate by 5.0–6.1% and by 7.2–8.2% at the corresponding pH levels, respectively (Fig. 2). UVA significantly ($p < 0.01$) enhanced the growth on the cloudy/rainy days, while UVB always resulted in inhibition regardless of the radiation levels.

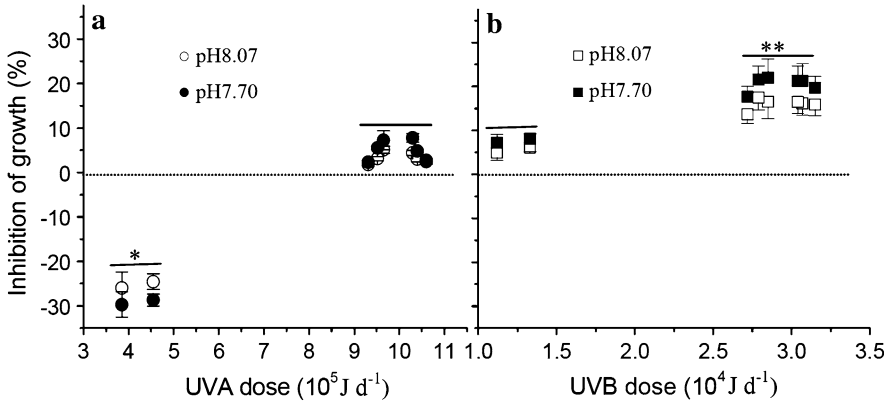

Fig. 2 Relative inhibition of the specific growth rate of *Phaeocystis globosa* induced by UVA (**a**) or UVB (**b**) at pH 8.07 (*open symbols*) or pH 7.70 (*solid symbols*) as a function of the UV dose. The inhibition of growth was calculated as μ_{Inh} (%) = $((\mu_P - \mu_{PA})/\mu_P) \times 100$ or $((\mu_{PA} - \mu_{PAB})/\mu_P) \times 100$, where μ_{Inh} represent UVA or UVB-induced inhibition to μ; μ_P, μ_{PA}, and μ_{PAB}, the specific growth rate (μ) of the cells grown under PAR alone, PAR + UVA and PAR + UVA + UVB treatments, respectively. The data represent the means ± SD in triplicate cultures ($n = 3$). * or ** indicate significant difference at $P < 0.05$ or $P < 0.01$ between the two pH levels

Photochemical activities

Under the ambient CO_2 and pH levels, the effective quantum yield ($\Delta F/F_m$) of *P. globosa* decreased from 0.66 at dawn to 0.168–0.322 (P), 0.146–0.295 (PA), and 0.121–0.245 (PAB) at noontime on the sunny days, and to 0.563–0.575 (P), 0.597–0.603 (PA) and 0.538–0.565 (PAB) on the cloudy/rainy days (Fig. 3a). When compared between the control and acidified conditions, the noontime yield in the low pH (high CO_2)-grown cells decreased by 14–17% (P), 16–20% (PA) and 19–24% (PAB) at day 1 and day 2 when it was sunny ($P < 0.05$), but increased by about 4–5% (P), 7–8% (PA) ($P < 0.05$) and 0% (PAB) at day 3 and 4 when it was cloudy and rainy (Fig. 3a). At day 8 (sunny) after about 26 generations, however, the acidification-induced reduction of the yield became insignificant ($P > 0.1$).

Non-photochemical quenching (NPQ) of chlorophyll fluorescence showed opposite pattern to that of the quantum yield, being higher on the sunny days and lower on the cloudy/rainy days (Fig. 3b). When compared between the ambient and the low pH cultures (the ratios of NPQ at the pH 7.70 to that at the pH 8.07), the acidification increased the NPQ by 3.6–8.6% (P), 5.2–12.1% (PA) and 6.1–17.1% (PAB) during noontime on the sunny days ($P < 0.05$), whereas it reduced them by 3.3–4.1% (P), 3.7–4.8% (PA) and 2.4-3.5% (PAB) on the cloudy/rainy days, respectively ($P < 0.05$).

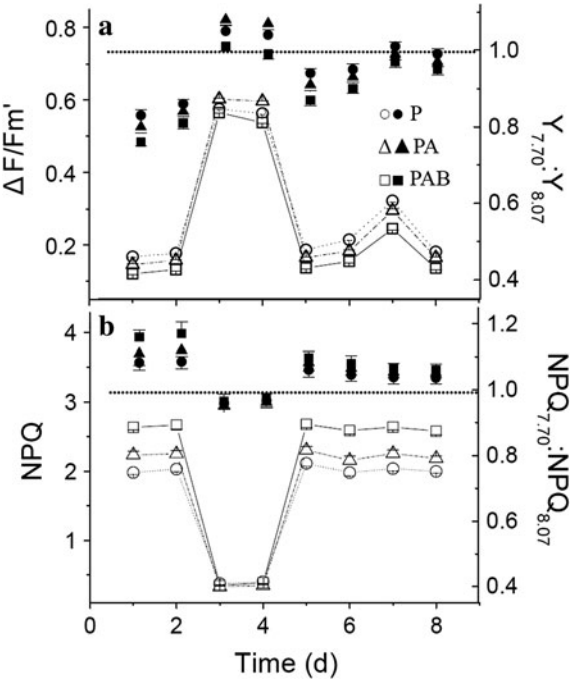

Fig. 3 Effective quantum yields ($\Delta F/F'_m$) (**a**) and non-photochemical quenching (NPQ) (**b**) measured at 12:00 AM (local noon) of *Phaeocystis globosa* grown at pH 8.07 (*open symbols*) and the ratios (*solid symbols*) of the yield or NPQ at pH 7.70 to that at pH 8.07 under P, PA, or PAB treatments, respectively. The data represent the means ± SD in triplicate cultures ($n = 3$)

When the photochemical parameters were plotted as a function of UV daily doses, UVA caused 8.4–14.9% inhibition of the yield at the high doses (the sunny days), while it brought about enhancement of the yield by 4.9–6.0% at the reduced dose levels (cloudy/rainy days). The acidification up-regulated the inhibition under the high UVA dose levels and down-regulated it under the low dose levels ($P < 0.05$) (Fig. 4a). At the high pH level, UVB caused 15.5–17.6% and 6.3–9.9% inhibition of the yield at the high and low dose levels, respectively, while it correspondingly induced 18.0–21.3 and 10.4–14.6% inhibition at the low pH ($P < 0.05$) (Fig. 4b). In view of the changes in NPQ, UVA increased it at the high doses but decreased it on the low dose levels (Fig. 4c), while UVB enhanced it at either the high or low dose levels (Fig. 4d). The CO_2-driven acidification significantly enhanced the NPQ by about 3–9% in the presence of UVR on the sunny days.

Photosynthesis, respiration, and carbonic anhydrase at different CO_2 (or pH) levels

When the high CO_2/low pH-grown cells were exposed to CO_2 levels of more than 25 μmol l^{-1}, their photosynthetic and respiratory rates were significantly ($P < 0.05$) higher than the ambient CO_2-grown cells (Fig. 5). The maximal net photosynthetic rate was 8.1% higher in the former than the latter if the rate measurements were normalized to Chl *a*, and up to 8.7% normalized to a cell. The $K_{m(CO_2)}$ values of the cells acclimated to the low and high CO_2 levels were 1.21 ± 0.42 and 1.50 ± 0.41 μmol l^{-1}, respectively, being insignificantly ($P > 0.1$) different. The dark respiration was 1.7–2.0% higher ($P < 0.05$) in the high-CO_2-grown cells than the ambient CO_2-grown cells.

The activity of extracellular and intracellular carbonic anhydrase (ECA and ICA) changed insignificantly under the acidified conditions compared to

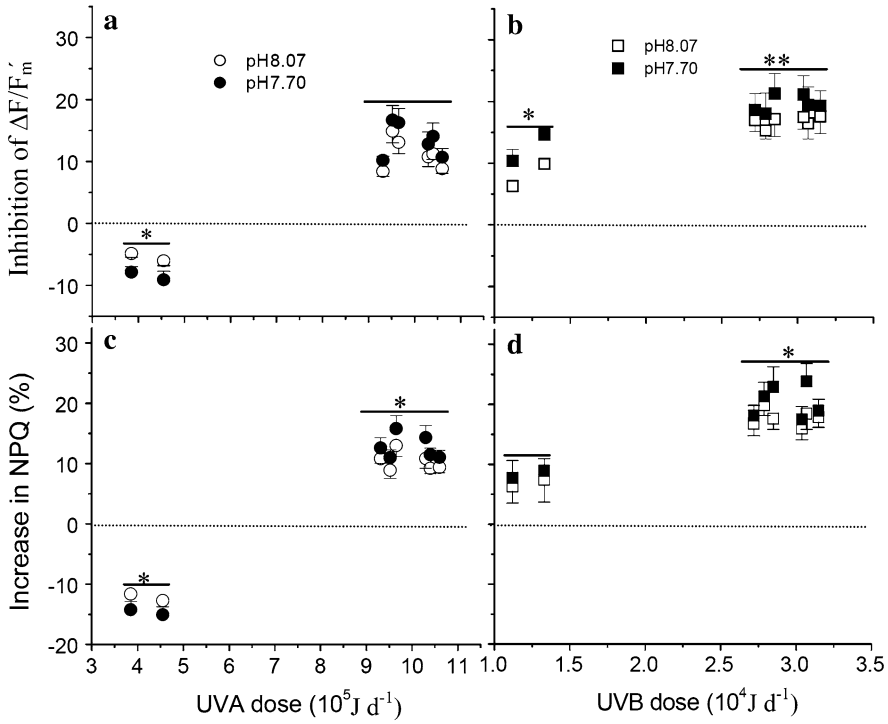

Fig. 4 UVA (*circle*) or UVB (*square*)-induced inhibition of the effective quantum yield ($\Delta F/F'_m$) (**a**, **b**) and non-photochemical quenching (NPQ) (**c**, **d**) of *Phaeocystis globosa* cells grown at pH 8.07 (*open symbols*) or pH 7.70 (*solid symbols*) as a function of the UV dose. The inhibition of $\Delta F/F_m$ was calculated as Y_{Inh} (%) $= ((Y_P - Y_{PA})/Y_P) \times 100$ or $((Y_{PA} - Y_{PAB})/Y_P) \times 100$; the increase in NPQ was calculated as N_{Inc} (%) $= ((N_{PA} - N_P)/N_P) \times 100$ or $(N_{PAB} - N_{PA})/N_P) \times 100$, where Y_{Inh} or N_{Inc} represent UVA or UVB-induced inhibition to Y or increase in NPQ; Y_P or N_P, Y_{PA} or N_{PA}, and Y_{PAB} or N_{PAB}, $\Delta F/F_m$ or NPQ of the cells grown under PAR alone, PAR + UVA and PAR + UVA + UVB treatments, respectively. The data represent the means ± SD ($n = 3$). * or ** indicate significant difference at $P < 0.05$ or $P < 0.01$ between the two pH levels

the ambient pH level (Fig. 6). Presence of UVR did not affect the activity of ICA (Fig. 6b), but it increased ($P < 0.05$) the activity of ECA by 2.5% at pH 8.07 and by 2.9% at pH 7.70 (Fig. 6c). UV-A did not result in significant change in the activity of ECA, reflecting the UVB-induced stimulation.

Pigments and UV absorptivity

The contents of Chl *a* increased by 9–12%, and that of Chl *c* increased by 4–10.3% (Fig. 7) in the high-CO_2-grown cells, regardless of the radiation treatments. Presence of UVR decreased the content of Chl *c* ($P < 0.05$), but brought insignificant ($P > 0.1$) change in Chl *a* content (Fig. 7a, b). The content of carotenoids increased by 7.0% (P), 8.7% (PA), and 10.6% (PAB) under the acidified condition, and both UVA and UVB stimulated the accumulation of carotenoids ($P < 0.05$) (Fig. 7c).

The absorptivity (peaked at 340 nm) of UVACs in *P. globosa* cells showed an insignificant ($P > 0.1$) change under the acidified conditions (Fig. 8a). Presence of UVA or UVB did not result in any significant difference in the absorptivity (Fig. 8b).

Discussion

The CO_2-induced acidification of seawater led to decreased PSII quantum yield and growth rate of *P. globosa* under high levels of solar PAR on the sunny days, and addition of UVA or UVB further deteriorated the impacts. However, during cloudy or rainy days with reduced levels of solar radiation, the enriched CO_2 and UVA acted synergistically to fuel

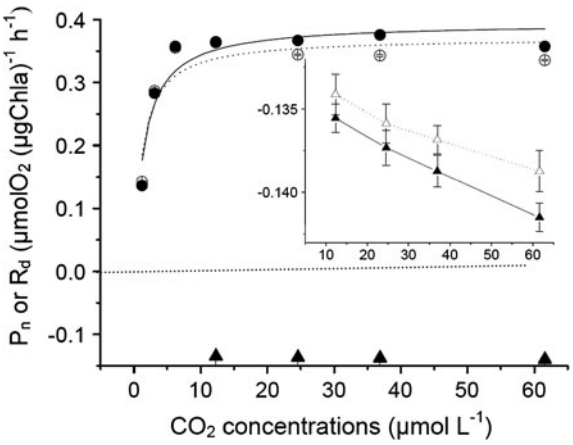

Fig. 5 The net photosynthetic rate (*circle*) and dark respiration (*triangle*) of *Phaeocystis globosa* cells grown at the low (*open*) and high CO_2 (*solid*) levles as a function of CO_2 concentrations. The corresponding pH levels at which the measurement was made in the CO_2 equilibrated medium were 8.82, 8.55, 8.34, 8.07, 7.80, 7.63, and 7.43, respectively. The data represent the means ± SD in triplicate cultures ($n = 3$). The *inset* is for the enlargement of the dark respiration change

the photochemical yield and growth rate. Low levels of UV irradiances are known to stimulate uptake of bicarbonate in a green microalga (Giraldez et al., 1998) and photosynthesis in phytoplankton assemblages (Gao et al., 2007b). An increase of CO_2aq and bicarbonate ions under the acidified condition could have raised the availability of the inorganic carbon and saved energy required for operation of the CCM. However, under the PAR-excessive conditions, UVR must have brought more damages to the photosynthetic machinery or resulted in less repairing of the damages under the acidified conditions, leading to higher photoinhibition and NPQ.

During the initial acclimation in contrast to the later phase (Figs. 1, 3), the acidification led to much lower growth rate and photochemical quantum yield and higher NPQ. A decrease in quantum yield of microalga, when transferred to high CO_2/low pH solution, was suggested to be caused by stimulated acidification in the stroma (Satoh et al., 2001). Such initial down-regulated quantum yield, however, disappears with declining activity of intracellular CA (Giordano et al., 2005) and increased activity ratio of PSI to PSII (Satoh et al., 2001). For *P. globosa*, however, acclimation to the high CO_2-induced acidification did not affect the activity of its extracellular or intracellular CA (Fig. 6), but resulted in an

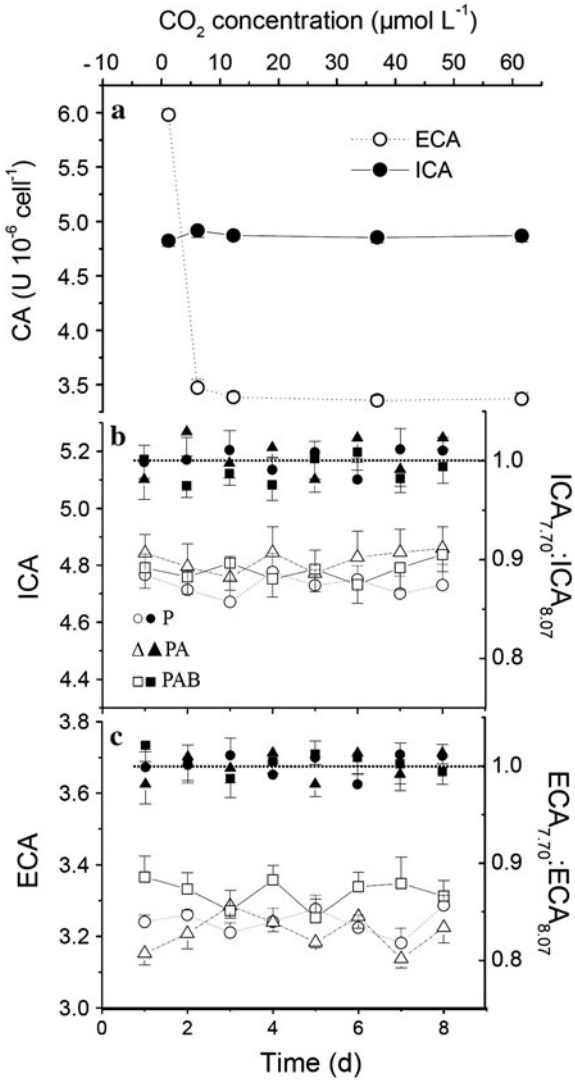

Fig. 6 **a** The acitivity of carbonic anhylase (CA) of *Phaeocystis globosa* grownt at different CO_2 levels for 3 days under indoor condition at 50 μmol photons m^{-2} s^{-1} (PAR)(12L:12D) and 15°C. The corresponding pH levels at different CO_2 concentrations were 8.82, 8.34, 8.07, 7.63, and 7.43, respectively. **b** Intracellular CA (ICA); **c** extracellular CA (ECA). Activity of ICA or ECA were shown for the cells grown at the low CO_2 or pH 8.07 (*open symbols*), the ratios (*solid symbols*) of the ECA or ICA at pH 7.70 to that at pH 8.07 were presented for the cells grown under different radiation treatments. The data represent the means ± SD in triplicate cultures ($n = 3$)

increase in the contents of Chl *a*, Chl *c*, and carotenoids (Fig. 7). This implies that the alga counteracted the acidification by acquiring additional energy via enlarging its antenna size and enhancing its photoprotective strategy.

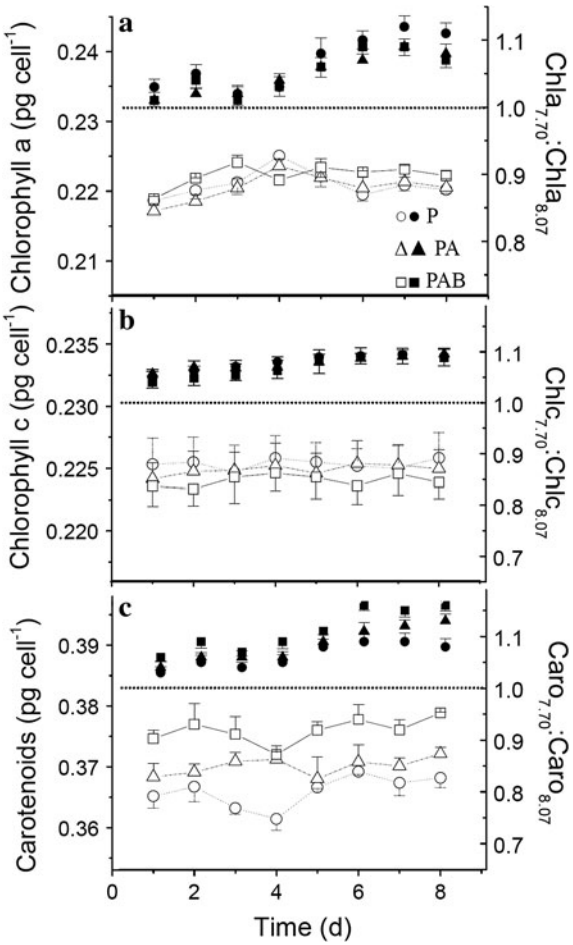

Fig. 7 Contents of chlorophyll *a* (**a**), chlorophyll *c* (**b**), and carotenoids (**c**) of *Phaeocystis globosa* cells grown at pH 8.07 (*open symbols*) and the ratios (*solid symbols*) of the contents at pH 7.70 to that at pH 8.07. The data represent the means ± SD ($n = 3$)

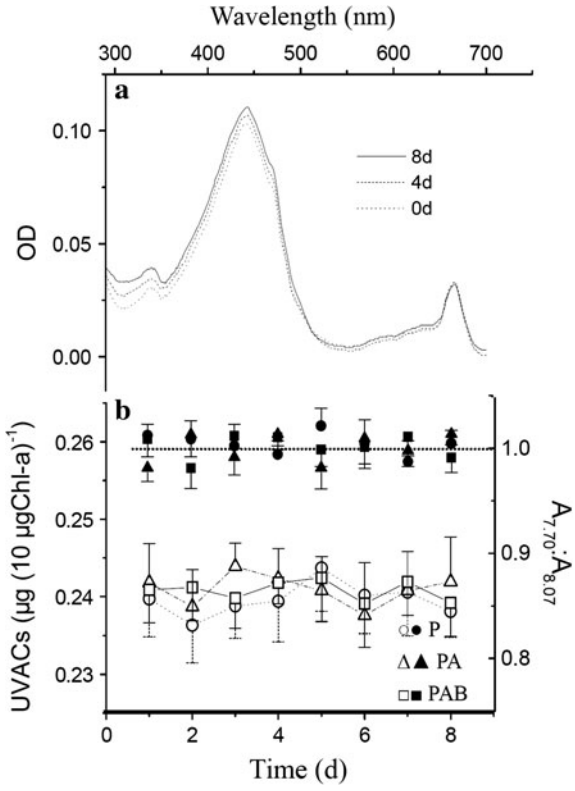

Fig. 8 **a** UV–visible light absorption spectra of absolute methanol extracts of *P. globosa* cells grown under full spectrum solar radiation and ambient CO_2 level (pH 8.07) air. The absorptivity of UV-absorbing compounds (UVACs) were normalized to the contents of chl *a*. **b** UVACs of the cells grown at pH 8.07 (*open symbols*) and the ratios (*solid symbols*) of the UVACs at pH 7.70 to that at pH 8.07 under different solar radiation treatments. The data represent the means ± SD in triplicate cultures ($n = 3$)

Elevated CO_2 concentration to 750 ppmv was shown to stimulate *P. globosa*'s growth rate under indoor low light conditions (Wang et al., 2010). In this study, effects of the CO_2-induced acidification on *P. globosa* under solar radiation were positive on cloudy days but negative on sunny days in the presence of UVR (Figs. 2, 4), reflecting a dependence on the quality and quantity of radiations. Elevated CO_2 level was shown to increase the sensitivity of the diatom *Thalassiosira pseudonana* and some freshwater phytoplankton to UVB or high PAR (Sobrino et al., 2008, 2009). This study showed additionally synergistic effects of UVA and the CO_2 enrichment on *P. globosa*. The enriched CO_2 increased photosynthetic performance under reduced levels of solar radiation in the presence of UVA or indoor PAR condition (Fig. 1, 3a), suggesting that the increased availability of CO_2 stimulated the energy-limited photosynthesis.

In this study, UVB acted synergistically with the acidification to reduce the photochemical efficiency and growth (Figs. 2b, 4b, d). However, moderate levels of UVA stimulated the photochemical efficiency and growth rate of *P. globosa* on the rainy/cloudy days (Figs. 1, 3), and such an enhancement was more pronounced in the low pH/high CO_2-grown cultures. Under PAR-limited conditions, presence of UVA can stimulate photosynthesis or CO_2-acquisition-related enzymes (Wu & Gao, 2009). UVA can also facilitate the repair of UVB-damaged molecules

(Dany et al., 2001, Krizek, 2004). Moderate levels of UVA were shown to stimulate the activity of the extracellular CA and synthesis of other periplasmic proteins in the diatom *Skeletonema costatum* (Wu & Gao, 2009). In addition, UVA was found to drive photosynthetic carbon fixation of phytoplankton in the absence of PAR (Gao et al., 2007b) or to enhance it under reduced levels of solar radiation (Helbling et al., 2003; Gao et al., 2007b). Under PAR-limited and CO_2-enriched conditions, addition of UVA could have ministered to photosynthetic machinery as well as Ci acquisition process in *P. globosa* by providing addition energy and stimulating activity of periplasmic enzymes.

The elevated pCO_2 and acidification did not significantly alter the activity of both intracellular and extracellular CA and resulted insignificant effect on the photosynthetic affinity for CO_2 in *P. globosa*, reflecting the insensitiveness of its CCM to the elevated CO_2 level. Most of the phytoplankton species studied so far, including *P. globosa*, showed CO_2 concentrating mechanisms (CCMs) (Giordano et al., 2005). Enrichment of CO_2 has been shown to down-regulate the CCMs (Raven & Beardall, 2003) and the energy demand for Ci acquisition process (Giordano et al., 2005; Beardall et al., 2009). Such down-regulation was found to be synchronized with the diurnal photosynthetic performance in the diatom *Skeletonema costatum* (Chen & Gao, 2004). However, in *P. globosa*, an increase of CO_2aq from 39 (12.5 μmol l^{-1}) to 101 Pa (32.4 μmol l^{-1}) did not affect its photosynthetic affinity for CO_2 or DIC (Fig. 5) and its extracellular CA or intracellular CA activity (Fig. 6). In another study by Rost et al. (2003), the CCM of this species was not down-regulated either under elevated CO_2 concentrations. The uptake rate of bicarbonate by *P. globosa* was not affected in the cells acclimated to a range of 1.2–58.3 μmol l^{-1} CO_2aq (Rost et al., 2003). The activity of CA, in the present study, was not influenced in the cells acclimated to 6–60 μmol l^{-1} CO_2aq, only at the CO_2aq level of 1.2 μmol l^{-1}, the activity of intracellular CA was stimulated (Fig. 6a). All these results imply that increasing pCO_2 to the projected level for the end of this century will not affect the CCM of *P. globosa*.

Interactive effects of UVR and the CO_2-induced seawater acidification on phytoplankton may differ from species to species. Since UVA and acidification may act synergistically to stimulate the growth under reduced levels of solar radiation, and both UVA and UVB may act together with acidification to reduce the photochemical yield and growth rate under high levels of solar radiation, the net or balanced effects of ocean acidification on primary producers would depend on the depth or mixing that alter the exposures of the phytoplankton cells in the water column to solar radiation. In the present study, the red tide alga *P. globosa* increased its NPQ and dark respiration under the CO_2-induced seawater acidification (Fig. 5), implying that increased acidity by 0.37 units of pH was a stress. Some diatoms showed enhanced growth rate with enriched CO_2 and acidity (Riebesell et al., 1993, Riebesell 2004; Sobrino et al., 2008; Wu et al., 2010). Although it is difficult to predict whether ocean acidification would reduce the frequency of HAB, it is certain that solar radiation interacts with ocean acidification to affect the physiological performance of *P. globosa*. Therefore, fluctuation of light and UV radiations will act differently in future high CO_2 oceans than today.

Acknowledgments This study was supported by National Basic Research Program of China (No. 2009CB421207), by program for Changjiang Scholars and Innovative Research Team (IRT0941) and by National Natural Science Foundation (No. 40930846, No. 40876058).

References

Anderson, D. H. & R. J. Robinson, 1946. Rapid electrometric determination of alkalinity of sea water using glass electrode. Industrial and Engineering Chemistry 18: 767–769.

Barry, J. P., T. Tyrrell, L. Hansson, G. Plattner & J. Gattuso, 2010. Atmospheric CO_2 targets for ocean acidification perturbation experiments. In Riebesell, U., V. J. Fabry, L. Hansson & J. Gattuso (eds), Guide to Best Practices in Ocean Acidification Research and Data Reporting. Luxembourg Press, Belgium: 53–64.

Beardall, J., P. Heraud, S. Roberts, K. Shelly & S. Stojkovic, 2002. Effects of UVB radiation on inorganic carbon acquisition by the marine microalga *Dunaliella tertiolecta* (Chlorophyceae). Phycologia 41: 268–272.

Beardall, J., C. Sobrino & S. Stojkovic, 2009. Interactions between the impacts of ultraviolet radiation, elevated CO_2, and nutrient limitation on marine primary producers. Photochemical & Photobiological Science 8: 125–1265.

Bilger, W. & O. Björkman, 1990. Role of the xanthophylls cycle in photoprotection elucidated by measurements of light-induced absorbance changes, fluorescence and photosynthesis in leaves of *Hedera canariensis*. Photosynthesis Research 25: 173–185.

Bouchard, J. N., D. A. Campbell & S. Roy, 2005. Effects of UVB radiation on the D1 protein repair cycle of natural

phytoplankton communities from three latitudes (Canada, Brazil and Argentina). Journal of Phycology 41: 273–286.

Buma, A. G. J., S. W. Wright & R. VandenEnden, 2006. PAR acclimation and UVBR-induced DNA damage in Antarctic marine microalga. Marine Ecology Progress Series 315: 33–42.

Burkhardt, S., G. Amoroso, U. Riebesell & D. Sueltemeyer, 2001. CO_2 and HCO_3^- uptake in marine diatom acclimated to different CO_2 concentrations. Limnology and Oceanography 46: 1378–1391.

Caldeira, K. & M. E. Wickett, 2003. Anthropogenic carbon and ocean pH. Nature 425: 365.

Chen, X. & K. Gao, 2004. Characterization of diurnal photosynthetic rhythms in the marine diatom *skeletonema costatum* grown in synchronous culture under ambient and elevated CO_2. Function Plant Biology 31: 399–404.

Dany, A. L., T. Douki, C. Triantaphylides & J. Cadet, 2001. Repair of the main UV-induced thymine dimeric lesions within *Arabidopsis thaliana* DNA: evidence for the major involvement of photoreactivation pathways. Journal of Photochemistry and Photobiology B 65: 127–135.

Dunlap, W. C., G. A. Rae & E. W. Helbling, 1995. Ultraviolet-absorbing compounds in natural assemblages of Antarctic phytoplankton. Antarctic Journal U. S. 30: 323–326.

Gao, K., Y. Aruga, T. Ishihara, T. Akano & M. Kiyohara, 1991. Enhanced growth of the red alga *Porphyra yezoensis* Ueda in high CO_2 concentrations. Journal of Applied Phycology 3: 355–362.

Gao, K., Y. Aruga, K. Asada, T. Ishihara, T. Akano & M. Kiyohara, 1993. Calcification in the articulated coralline alga *Corallina pilufera*, with special reference to the effect of elevated CO_2 concentration. Marine Biology 117: 129–132.

Gao, K., W. Guan & E. W. Helbling, 2007a. Effects of solar ultraviolet radiation on photosynthesis of the marine red tide alga *Heterosigma akashiwo* (Raphidophyceae). Journal of Photochemistry and Photobiology B 86: 936–951.

Gao, K., Y. Wu, G. Li, H. Wu, V. E. Villafane & E. W. Helbling, 2007b. Solar UV radiation drives CO_2 fixation in marine phytoplankton: A double-edged sword. Plant Physiology 144: 54–59.

Gao, K., P. Li, T. Watanabe & E. W. Helbling, 2008. Combined effects of ultraviolet radiation and temperature on morphology, photosynthesis, and DNA of *Arthrospira (Spirulina) platensis* (CYANOPHYTA). Journal of Phycology 3: 777–786.

Gao, K., Z. Ruan, V. E. Villafane, J. Gattuso & E. W. Helbling, 2009. Ocean acidification exacerbates the effect of UV radiation on the calcifying of phytoplankter *Emiliania huxleyi*. Limnology and Oceanography 54: 186–1855.

Gattuso, J. & H. Lavigne, 2010. Perturbation experiments to investigate the impact of ocean acidification: approaches and software tools. Biogeoscience Discussion 6: 4413–4439.

Genty, B., J. M. Briantais & N. R. Baker, 1989. The relationship between the quantum yield of photosynthetic electron transport and quenching of chlorophyll fluorescence. Biochemistry and Biophysiology Acta 990: 87–92.

Giordano, M., J. Beardall & J. A. Raven, 2005. CO_2 concentration mechanisms in algae: mechanisms, environmental modulation, and evolution. Annual Review of Plant Biology 56: 99–131.

Giraldez, N., P. J. Aparicio & M. A. QuiAones, 1998. Blue light requirement for HCO_3^- uptake and its action spectrum in *Monoraphidium braunii*. Photochemistry and Photobiology 68: 420–426.

Häder, D. P., M. Lebert, R. Marangoni & G. Colombetti, 1999. ELDONET-Euopean light dosimeter network hardware and software. Journal of Photochemistry and Photobiology B 52: 51–58.

Hein, M. & K. Sand-Jensen, 1997. CO_2 increases oceanic primary production. Nature 388: 526–527.

Helbling, E. W., K. Gao, J. G. Rodrigo, H. Wu & V. E. Villafane, 2003. Utilization of solar UV radiation by coastal phytoplankton assemblages off SE China when exposed to fast mixing. Marine Ecology Progress Series 259: 59–66.

Hoegh-Guldberg, O., P. J. Mumby, A. J. Hooten & R. S. Steneck, 2007. Coral reefs under rapid climate change and ocean acidification. Science 318: 1737–1742.

Krizek, D. T., 2004. Influence of PAR and UVA in determining plant sensitivity and photomorphogenic responses to UVB radiation. Photochemistry and Photobiology 79: 307–315.

LaRoche, J., B. Rost & A. Engel, 2010. Bioassays, batch culture and chemostat experimentation. In Riebesell, U., V. J. Fabry, L. Hansson & J. Gattuso (eds), Guide to Best Practices in Ocean Acidification Research and Data Reporting. Luxembourg Press, Belgium: 81–94.

Lesser, M. P., 2008. Effects of ultraviolet radiation on productivity and nitrogen fixation in the cyanobacterium, *Anabaena* sp. (Newton's strain). Hydrobiologia 598: 1–9.

Lewis, E. & D. W. R. Wallace, 1998. Program developed for CO_2 system calculations. ORNL/CDIAC-105. Carbon Dioxide Information Analysis Center, Oak Ridge National Laboratory, U.S. Department of Energy [available on internet at http://cdiac.ornl.gov/oceans/CO2rprt.html]. Accessed 12 June 2007.

Munday, P. L., D. L. Dixson & J. M. Donelson, 2009. Ocean acidification impairs olfactory discrimination and homing ability of a marine fish. Proceeding of Royal society B 276: 3275–3283.

Orr, J. C., V. J. Fabry, O. Aumont, L. Bopp & S. C. Doney, 2005. Anthropogenic ocean acidification over the twenty-first century and its impact on calcifying organisms. Nature 437: 681–686.

Peperzak, L. & M. Poelman, 2008. Mass mussel mortality in the Netherlands after a bloom of *Phaeocystis globosa* (prymnesiophyceae). Journal of Sea Research 60: 220–222.

Qi, Y., J. Chen, Z. Wang, N. Xu, Y. Wang, P. Shen, et al., 2004. Some observations on harmful algal bloom (HAB) events along the coast of Guangdong, southern China in 1998. Hydrobiologia 512: 209–214.

Raven, J. A. & J. Beardall, 2003. Carbon acquisition mechanisms of algae: carbon dioxide diffusion and carbon dioxide concentration mechanisms. In Larkum, A. W. D., S. E. Douglas & J. A. Raven (eds), Advances in Photosynthesis and Respiration, Vol. 14: Photosynthesis in Algae. Kluwer, Dordrecht: 225–244.

Riebesell, U., 2004. Effects of CO_2 enrichment on marine phytoplankton. Journal of Oceanography 60: 719–729.

Riebesell, U., D. A. Wolf-Gladrow & V. Smetacek, 1993. Carbon dioxide limitation of marine phytoplankton growth rates. Nature 361: 249–251.

Riebesell, U., I. Zondervan, B. Rost, P. D. Tortell, R. E. Zeebe & F. M. M. Morel, 2000. Reduced calcification of marine plankton in response to increased atmospheric CO_2. Nature 407: 364–367.

Riebesell, U., K. G. Schulz, R. G. J. Bellerby, M. Botros, P. Fritsche, M. Meyerhöfer, C. Neill, G. Nonda, A. Oschlies, J. Wohlers & E. Zöllner, 2007. Enhanced biological carbon consumption in a high CO_2 ocean. Nature 450: 545–548.

Rilegman, R. & W. V. Boekel, 1996. The ecophysiology of *phaeocystis globosa*: a review. Journal of Sea Research 35: 235–242.

Rost, B., U. Riebesell, S. Burkhardt & D. Sueltemeyer, 2003. Carbon acquisition of bloom-forming marine phytoplankton. Limnology and Oceanography 48: 55–67.

Rousseau, V., M. Chretiennot-Dinet, A. Jacobsen, P. Verity & S. Whipple, 2007. The life cycle of *Phaeocystis*: state of knowledge and presumptive role in ecology. Biogeochemistry 83: 29–47.

Satoh, A., N. Kurano & S. Miyachi, 2001. Inhibition of photosynthesis by intracellular carbonic anhydrase in microalga under excess concentrations of CO_2. Photosynthesis Research 68: 215–224.

Schippers, P., M. Lürling & M. Scheffer, 2004. Increase of atmospheric CO_2 promotes phytoplankton productivity. Ecology Letters 7: 446–451.

Schmidt, E. C., M. Maraschin & Z. L. Bouzon, 2010. Effects of UVB radiation on the carragenophyte *Kappaphycus alvarezii* (Rhodophyta, Gigartinales). Hydrobiologia 649: 171–182.

Schoemann, V., S. Becquevort, J. Stefels, V. Rousseau & C. Lancelot, 2005. *Phaeocystis* blooms in the global ocean and their controlling mechanisms: a review. Journal of Sea Research 53: 43–66.

Sobrino, C., P. J. Neale & L. M. Lubian, 2005. Interaction of UV radiation and inorganic carbon supply in the inhibition of photosynthesis: spectral and temporal response of two marine picoplankton. Journal of Photochemistry and Photobiology B 81: 384–393.

Sobrino, C., M. L. Ward & P. J. Neale, 2008. Acclimation to elevated carbon dioxide and ultraviolet radiation in the diatom *Thalassiosira pseudonana*: effects on growth, photosynthesis, and spectral sensitivity of photoinhibition. Limnology and Oceanography 53: 494–505.

Sobrino, C., P. J. Neale, J. D. Phillips-Kress, R. E. Moeller & J. Porter, 2009. Elevated CO_2 increases sensitivity to ultraviolet radiation in lacustrine phytoplankton assemblages. Limnology and Oceanography 54: 2448–2459.

Tortell, P. D., G. R. Ditullio, D. M. Sigmann & F. M. M. Morel, 2002. CO_2 effects on taxonomic composition and nutrient utilization in an Equatorial Pacific phytoplankton assemblage. Marine Ecology Progress Series 236: 37–43.

Wang, Y., W. O. Smith Jr., X. Wang & S. Li, 2010. Subtle biological responses to increased CO_2 concentrations by *Phaeocystis globosa* Scherffel, a harmful algal bloom species. Geophysical Research Letters 37: L09604.

Wellburn, A. R., 1994. Spectral determination of chlorophylls a and b, as well as total Carotenoids, using various solvents with spectrophotometers of different resolution. Journal of plant physiology 144: 307–313.

Wu, H. & K. Gao, 2009. UV radiation-stimulated activity of extracellular carbonic anhydrase in the marine diatom *Skeletonema costatum*. Functional Plant Biology 36: 137–143.

Wu, Y. P., K. Gao & U. Riebesell, 2010. CO_2-induced seawater acidification affects physiological performance of the marine diatom *Phaeodactylum tricornutum*. Biogeosciences 7: 2915–2923.

Ye, C., K. Gao & M. Giordano, 2008. The odd behaviour of carbonic anhydrase in the terrestrial cyanobacterium *nostoc flagelliforme* during hydration dehydration cycles. Environmental Microbiology 10: 1018–1023.

Zheng, Y. & K. Gao, 2009. Impacts of solar UV radiation on the photosynthesis, growth, and UV-absorbing compounds in *Gracilaria lemaneiformis* (RHODOPHYTA) grown at different nitrate concentration. Journal of Phycology 45: 314–323.